2023 IEEE International Conference on Robotics and Automation (ICRA 2023)
May 29 - June 2, 2023. London, UK

Extremum Seeking-Based Adaptive Sliding Mode Control with Sliding Perturbation Observer for Robot Manipulators

Hamza Khan, and Min Cheol Lee, *Member, IEEE*

***Abstract*— This paper proposed an adaptive robust sliding mode control (SMC) with a nonlinear sliding perturbation observer (SPO) for robot manipulators. SPO estimates the perturbation (nonlinearities, uncertainties, and disturbances) with minimal system information and enhances the controller performance. The estimation is mainly dependent on the selection of SMCSPO gain, and if not tuned well, it might result in increased error dynamics of the system. Therefore, minimizing the error dynamics by improving the estimation is the primary goal of this research. In this regard, the current study accomplishes adaptation of controller gain in real-time by using an optimization technique called extremum seeking (ES). The quality adaptation is controlled with the help of a cost function. Based on the Lyapunov-based stability analysis of SMCSPO, the cost function consisting of the estimation error of the observer and error dynamics is proposed. The unique cost function now guarantees the tracking performance within the defined error tolerance. The effectiveness of the proposed algorithm is illustrated and validated in simulation and experiments. It is shown that the adaptation based on ES with the proposed cost function converges to the optimal control gain enabling the reduced estimation error and error dynamics with enhanced tracking performance.**

I. Introduction

This research is conducted for the control of multi-degree-of-freedom (DOF) robot manipulators. This research aims to enhance the accuracy of industrial applications such as parts assembling or material cutting [1]. Hence, precise trajectory tracking is the prime concern that can be attained through robust control algorithms. For robust control of the multi-DOF robot manipulator, a robust nonlinear control algorithm known as sliding mode control (SMC) with sliding perturbation observer (SPO) (SMCSPO) was utilized by fellow researchers [2]. SMCSPO is a perturbation observer-based SMC that utilizes the partial state feedback (position only) to estimate the system states and the perturbation (nonlinearities, uncertainties, and disturbances) with considerable accuracy. Subsequently, the estimated perturbation is compensated from the system response to enhance the trajectory tracking performance and eliminate the chattering phenomena of SMC.

The quality of estimation depends upon the selection of control SMCSPO parameters. Effectively selecting these parameters significantly contributes to the high-precision motion and accurate trajectory tracking performance but may limit the effectiveness if poorly tuned. Therefore, in the presence of system dynamics and perturbation, the SMC parameter's optimal tuning process can be achieved by adapting to different sliding conditions. Two approaches [3] have been considered for the systems with upper bound unknown perturbation for adaptive SMC. The first strategy consists of increasing and decreasing the gains ensuring the finite-time convergence of sliding variables to some neighborhood of zeros. But this depends on the upper bound of perturbation, which doesn't guarantee the sliding mode will never be lost. The second adaptation strategy is model-based, which employs equivalent control of SMC to estimate disturbance. But, in this case, it is generally assumed that the system's exact model is challenging to calculate, and therefore, the estimation may not be accurate. Likewise, fuzzy logic-based adaptive law requires good system knowledge to make fuzzy membership functions, and the heuristic approach may result in slow optimization because of higher calculation time [4].

Considering the challenges mentioned above, the suitable method for adaptive SMC is a model-free adaptation, intelligent adaptation, and observer-based adaptive SMC. H. Wang *et al.* and Y. Wang *et al.* presented a model-free adaptive sliding mode control that first estimates the unknown dynamics by using the time delay estimation method [5], [6]. However, the control input of SMC in experiments shows chattering, which in the current study is unacceptable. H. Razmi *et al.* and Z. Chen *et al.* presented neural network-based adaptive SMC [7] and radial basis function neural network-based adaptive SMC [8]. The adaptation and results show good performance. However, the system is relatively small compared to the industrial robot in the current study. Furthermore, the neural network-based adaptation requires higher training time. R-D Xi *et al.,* on the other hand, presented adaptive SMC with disturbance observer for robust control of robot manipulator [9]. The advantage of observer-based adaptive SMC is that it guarantees robustness by diminishing the influence of the lumped disturbances. Similarly, C. Jing *et al.* also proved the effectiveness of observer-based adaptive SMC [10]. The study concluded that the finite time stability and specific quality of the tracking performance can be achieved with a disturbance observer.

Considering the literature, this paper combines a model-free adaptive technique with observer-based SMC (SMCSPO) for robust manipulator control. Consequently, the observer will estimate the perturbation and compensate their effect from the system response. Model-free adaptation will optimally tune the controller to achieve practical finite-time stability and enhanced tracking performance. Therefore, to optimally tune the SMCSPO parameters, an adaptive law using a perturbation-based extremum seeking (ES) algorithm [11] in robot joint-space is proposed. The motivation for using ES is

*Research supported by research grant of Pusan National University and Korea Institute of Machinery and Material (NK238A, 2022, Korea).

All the authors are with the School of Mechanical Engineering, Pusan National University, Busan, South Korea. (e-mail: hamzakhan.0496@gmail.com, mclee@pusan.ac.kr).

its simple and model-free structure for real-time optimization problems, allowing fast adaptation [12]. The theoretical analysis then shows that the sliding surface dynamics of SMCSPO have the effect of estimated perturbation rather than the actual perturbation itself, making adaptation easy and optimal.

Moreover, Lyapunov-based stability analysis is performed, establishing a relationship between error dynamics, estimated perturbation error, and tuned SMCSPO parameters (presented in Section III). Subsequently, using the relationship between the abovementioned parameters, a novel cost function is proposed that controls the adaptation to balance the tracking performance and perturbation estimation. Simulation and experiments were performed to evaluate the effectiveness of the proposed algorithms. The results show that with the adaptation of the SMCSPO parameter, the perturbation estimation is enhanced, eventually reducing tracking error. So, the main contribution of this paper can be summarized as follows.

- Detailed stability analysis of SMCSPO with ES-based control parameter.
- Proposing a cost function with state estimation and error dynamics tends to enhance the observer estimation and tracking performance.

The paper is arranged as follows: Section 2 presents the formulation of the SMCSPO control algorithm. Section 3 formulates the ES algorithm and controller stability analysis. Section 4 discusses the simulation and experimental results, whereas section 5 concludes the proposed algorithm and results.

II. PRELIMINARIES

A. Control Problem Formulation

The ultimate goal is to design a nonlinear controller for multi-DOF systems with high tracking precision. Generally, a second-order dynamics for the *n*-th DOF manipulator [13] is given as

$$\ddot{x}_j = f_j(x) + \Delta f_j(x) + \sum_{i=1}^{n}\left[(b_{ji}(x) + \Delta b_{ji}(x))u_i\right] + d_j(t) \qquad j = 1, \dots, n \quad (1)$$

where $x \triangleq [X_1 \dots X_n]^T$ represents the state vector, $f_j(x)$ and $\Delta f_j(x)$ are the linear dynamic terms and dynamics uncertainties, respectively. $b_{ji}(x)$ and $\Delta b_{ji}(x)$ are the control gain matrix and their uncertainties, respectively. where u_i and d_j are the control input and external disturbance, respectively. The perturbation (ψ) of the system is the combination of system nonlinearities, dynamics uncertainties, and disturbances. Thus, the perturbation is written as

$$\psi_j(x,t) = \Delta f_j(x) + \sum_{i=1}^{n}\left[\Delta b_{ji}(x)u_i\right] + d_j(t) \quad (2)$$

It is *assumed* that perturbation is bounded by a known continuous function as

$$\Gamma_j(x,t) = F_j(x) + \sum\left|\Phi_j(x)u_i\right| + D_j(t) > \left|\psi_j(t)\right| \quad (3)$$

where $\Gamma_j(x,t)$ is the upper-bound of the perturbation, $F_j(x) > \left|\Delta f_j\right|$, $\Phi_j > \left|\Delta b_j\right|$and $D_j > \left|\psi_j(t)\right|$ represent the expected (unknown) upper bounds of the uncertainties. The structure of SMCSPO requires linear/minimal system information. Therefore, the linear parameters of the system were obtained using a technique known as the signal compression method (SCM) [2]. These parameters decouple and linearize (1) as

$$\ddot{x}_j = \frac{u_j}{J_j} - \frac{B_j}{J_j}\dot{x}_j + \psi_j(x,t) \qquad j = 1, \dots, n \quad (4)$$

where J_j and B_j are decoupled (linear) inertia and damping of each link (DOF). The coupled and nonlinear terms become the perturbation. Hence, the SMCPSO goal is to drive x to $x_d \triangleq \left[X_{d,1} \dots X_{d,n}\right]^T$ with $\psi_j(x,t)$ estimation such that the estimation error ($\tilde{\psi} = \hat{\psi} - \psi$) converges towards zero. Throughout the text, "*j*" in subscript shows the number of starting from one and ending at maximum DOF (*n*).

B. SMCSPO Formulation

For SMCSPO, (1) is decoupled for the control variable as (5) with a new control input $\bar{u}$ to compensate for the effect of perturbation from the system response

$$f_j(x) + \sum_{i=1}^{n} b_{ji}(x)u_i = \alpha_{3j}\bar{u}_j \quad (5)$$

where α_{3j} is an arbitrary positive gain. So, the overall control input (u) can also be expressed as

$$u = B^{-1}\mathrm{Col}[\alpha_{3j}\bar{u}_j - f_j(\hat{x})] \quad (6)$$

where $u = [u_1 \dots u_n]^T$, $B = [b_{ji}(\hat{x})]_{nxn}$ and Col represents the column vector. Now the system dynamics in (4) can be written as

$$\ddot{x}_j = \alpha_{3j}\bar{u}_j + \psi_j(x,t) \quad (7)$$

And the state space model of (7) is then expressed as

$$\begin{aligned} \dot{x}_{1j} &= x_{2j} \\ \dot{x}_{2j} &= \alpha_{3j}\bar{u}_j + \psi_j(x,t) \\ y_j &= x_{1j} \end{aligned} \quad (8)$$

Sliding Perturbation Observer.

Initially, the SPO is formulated because the dynamics of SPO are then utilized in SMC to evaluate the control and sliding dynamics. The structure of SPO is briefly discussed in [14] and can be written in terms of the estimation states as

$$\dot{\hat{x}}_{1j} = \hat{x}_{2j} - k_{1j}\cdot\mathrm{sat}(\tilde{x}_{1j}) - \alpha_{1j}\tilde{x}_{1j} \quad (9)$$

$$\dot{\hat{x}}_{2j} = -k_{2j}\cdot\mathrm{sat}(\tilde{x}_{1j}) + \alpha_{3j}\bar{u}_j - \alpha_{2j}\tilde{x}_{1j} + \hat{\psi}_j \quad (10)$$

$$\dot{\hat{x}}_{3j} = \alpha_{3j}^2(\alpha_{3j}\hat{x}_{2j} + \bar{u}_j - \hat{x}_{3j}) \quad (11)$$

$$\hat{\psi}_j = \alpha_{3j}(\alpha_{3j}\hat{x}_{2j} - \hat{x}_{3j}) \quad (12)$$

where $k_1, k_2, \alpha_3, \alpha_1$ and α_2 are the positive constants. The components with "^" represent the estimated states, whereas "∼" represents the error between actual and the estimated states. $\hat{x}_1$ and $\hat{x}_2$ are the state of the sliding observer representing the estimated position and velocity (in a revolute joint case, joint angle, and angular velocity), respectively. $\hat{x}_3$ is a new state variable to estimate the perturbation and $\tilde{x}_1 = \hat{x}_1 - x_1$. Now the observer error dynamics are obtained by subtracting the states in (8) from (9) and (10) as

$$\dot{\tilde{x}}_{1j} = \tilde{x}_{2j} - k_{1j}\cdot\mathrm{sat}(\tilde{x}_{1j}) - \alpha_{1j}\tilde{x}_{1j} \quad (13)$$

$$\dot{\tilde{x}}_{2j} = -k_{2j} \cdot \text{sat}(\tilde{x}_{1j}) - \alpha_{2j}\tilde{x}_{1j} + \tilde{\psi}_j \quad (14)$$

where $\text{sat}(\tilde{x}_{1j})$ is the saturation function and is defined as

$$sat(\tilde{x}_{1j}) = \begin{cases} \tilde{x}_{1j}/|\tilde{x}_{1j}| & \text{if } |\tilde{x}_{1j}| > \varepsilon_{oj} \\ \tilde{x}_{1j}/\varepsilon_{oj} & \text{if } |\tilde{x}_{1j}| \le \varepsilon_{oj} \end{cases} \quad (15)$$

where ε_{oj} is the boundary layer manifold for $\tilde{x}_{1j}$. When the sliding starts such that $\tilde{x}_{1j} = 0$ and $|\tilde{x}_{1j}| \le \varepsilon_{oj}$, and solving (13) and (14) together, the resulting error dynamics becomes

$$\dot{\tilde{x}}_{2j} + (k_{2j}/k_{1j})\,\tilde{x}_{2j} = \tilde{\psi}_j \quad (16)$$

(16) is a filter between $\tilde{\psi}$ and $\tilde{x}_{2j}$ with a cutoff frequency k_{2j}/k_{1j}. Now in SPO dynamics, the α_{3j} and k_{2j}/k_{1j} must be selected large enough to maximize the attenuation from actual perturbation to $\tilde{x}_{2j}$. And for better estimation, *the* $\tilde{x}_{2j}$ is desired to be as small as possible. The selection of constant is explained later in this section.

Sliding Mode Control

For the SMCSPO, the estimated sliding surface is taken as

$$\hat{s}_j = \dot{\hat{e}}_j + c_j \cdot \hat{e}_j \quad (17)$$

where $\hat{e}$ is the estimated joint position error $\hat{e} = \hat{x}_1 - x_d$ and c_j is a positive constant. For robust control with perturbation compensation, $\overline{u}$ is appropriately generated to enforce the sliding condition as $\hat{s}_j \cdot \dot{\hat{s}}_j \le 0$. Therefore, the $\dot{\hat{s}}_j$ is written as

$$\dot{\hat{s}}_j = -K_j \cdot \text{sat}(\hat{s}_j) \quad (18)$$

Expanding the saturation function as

$$\text{sat}(\hat{s}_j) = \begin{cases} \hat{s}_j/|\hat{s}_j| & \text{if } |\hat{s}_j| > \varepsilon_{cj} \\ \hat{s}_j/\varepsilon_{cj} & \text{if } |\hat{s}_j| \le \varepsilon_{cj} \end{cases} \quad (19)$$

where ε_{cj} is the boundary layer manifold for $\hat{s}_j$. Now. Taking the derivative of (17) with expanded $\hat{e}$ expression and substituting the previously discussed dynamics in the derivative and solving (see stability analysis) will result in the following relation

$$\dot{\hat{s}}_j = \alpha_{3j} \cdot \overline{u} - \tilde{x}_{1j}\left\{\frac{k_{2j}}{\varepsilon_{oj}} + \frac{c_j \cdot k_{1j}}{\varepsilon_{oj}} - \frac{k_{1j}^2}{{\varepsilon_{oj}}^2}\right\} - \left\{\frac{k_{1j}}{\varepsilon_{oj}}\right\}\tilde{x}_{2j} + c_j\{\hat{x}_{2j} - \dot{x}_{dj}\} - \ddot{x}_{dj} + \hat{\psi}_j \quad (20)$$

To enforce (18) when $\tilde{x}_{2j} = 0$, the control law is selected as (21) from (20) and (18)

$$\overline{u} = \frac{1}{\alpha_{3j}}\Big[-K_j \cdot \text{sat}(\hat{s}_j) + \tilde{x}_{1j}\left\{\frac{k_{2j}}{\varepsilon_{oj}} + \frac{c_j \cdot k_{1j}}{\varepsilon_{oj}} - \frac{k_{1j}^2}{{\varepsilon_{oj}}^2}\right\} - c_j\{\hat{x}_{2j} - \dot{x}_{dj}\} + \ddot{x}_{dj} - \hat{\psi}_j\Big] \quad (21)$$

It is clear from (21), that the perturbation is subtracted in the $\overline{u}$. (21) is then substituted in (6) to get the perturbation compensated control input for the system. (21) is substituted in (20) and results in the sliding surface dynamics as

$$\dot{\hat{s}}_j = -K_j \cdot \text{sat}(\hat{s}_j) - (k_{1j}/\varepsilon_{oj})\,\tilde{x}_{2j} \quad (22)$$

The coefficients for SMCSPO are selected based on the following relation [9]

$$\frac{k_{1j}}{\varepsilon_{oj}} = 3\lambda_d,\ \frac{k_{2j}}{k_{1j}} = \lambda_d,\ \alpha_{3j=}\sqrt{\frac{\lambda_d}{3}},\ c_j = \frac{K_j}{\varepsilon_{cj}} = \lambda_d \quad (23)$$

λ_d is the desired controller parameter that must be selected significantly large to yield higher attenuation of the perturbation resulting in better estimation and performance. The optimal selection of λ_d will place the poles of the closed loop system on the desired naturally stable location. Manually tuning might not be effective or a tedious task. Therefore, the selection of λ_d is done using some adaptation in real-time that will converge $\tilde{x}_{2j}$ towards zero.

III. Proposed Algorithm

A. Perturbation-Based Extremum Seeking

Extremum seeking (ES) is a non-model-based real-time optimization algorithm for nonlinear problems where the system's accurate dynamic information is not available. The object of ES is to minimize (in this research) an appropriately defined cost function $J(.)$ for the closed-loop system without knowing a priori extremum ($\lambda_d{}^*$) of ES objective. A well-known ES algorithm is perturbation-based ES [4]. The structure of perturbation-based ES is presented in Fig. 1.

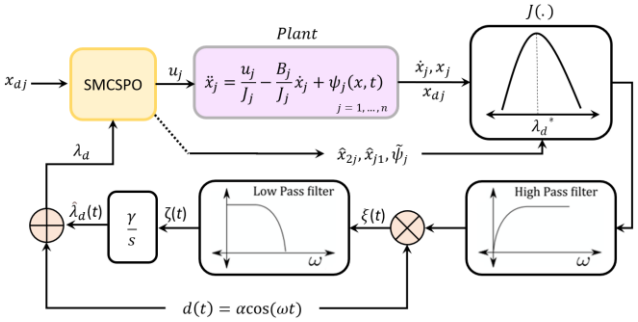

Figure 1. ES block diagram

In perturbation-based ES, periodic excitation signals with modulation frequency (ω) are used to estimate the gradient of the λ_d. In Fig. 1, the $d(t) = \alpha\cos(\omega t)$ is the dither signal, which presents a periodic perturbation signal with step size (α). The perturbation is added to the current best estimate of λ_d that is $\hat{\lambda}_d$. The controller is then updated with the new value of λ_d to modulate the system response. The system's actual and estimated states are then used in the cost function (explained later in cost function selection). The output of the cost function is then high pass filtered (HPF) to remove the dc components (η). The output of HPF is demodulated by multiplying the perturbation signal. The demodulated signal (ξ) is then low pass filtered (LPF), which generates a proportional gradient signal (ζ) using the cost function $J(.)$ information. The gradient signal is then integrated with gain γ to generate the estimated parameter ($\hat{\lambda}_d$). In the ES algorithm, the following assumptions are generally made.

1. The closed-loop dynamics are faster than the ES adaptation dynamics. Subsequently, the system is

exponentially stable for all $\lambda_d \in I$, where I is the range of stable parameters.

2. There is a unique optimum λ_d, represented by $\lambda_d{}^*$, of the convex cost function $J(.)$.

The current system was operated in discrete time (sampling time based). Therefore, the dynamic structure [11] of ES in Fig.1, in discrete form can be written as

$$\zeta(k) = -h\zeta(k-1) + J(k-1) \quad (24)$$

$$\hat{\lambda}_d(k+1) = \hat{\lambda}_d(k) + \gamma\alpha\cos(\omega k)[J(k) - (1+h)\zeta(k)] \quad (25)$$

$$\lambda_d(k+1) = \hat{\lambda}_d(k+1) + \alpha\cos(\omega \cdot (k+1)) \quad (26)$$

where γ, α are the adaptation gain and the perturbation amplitude, respectively. ω is the modulation frequency and is selected as $\omega = a\pi: 0 < a < 1$. Furthermore, the HPF $(descritized\ form: (z-1)/(z+h))$ is designed using the constant $0 < h < 1$ and a cutoff frequency below the modulation frequency. The stability and convergence of ES are mainly influenced by the selection of γ, and α. But very low γ will slower the adaptation, and very high γ will diverge the system from the optimal solution.

B. Convergence and Stability Analysis

SMCSPO

For a stable closed-loop system, SMCSPO will ensure $\hat{s}_j \cdot \dot{\hat{s}}_j \leq 0$. The Lyapunov function is selected as $V = \hat{s}_j \cdot \dot{\hat{s}}_j < 0$. Therefore, the estimated sliding surface in (17) can also be written as

$$\hat{s}_j = (\dot{\hat{x}}_{1j} - \dot{x}_{dj}) + c_j \cdot (\hat{x}_{1j} - x_{dj}) \quad (27)$$

Substituting (9) in (27) with $\alpha_{1j} = 0$ will yield

$$\hat{s}_j = (\hat{x}_{2j} - k_{1j} \cdot \mathrm{sat}(\tilde{x}_{1j}) - \dot{x}_d) + c_j \cdot (\hat{x}_{1j} - x_{dj}) \quad (28)$$

After reaching phase $\tilde{x}_{1j} = 0$, (28) will take the following form

$$\hat{s}_j = (\hat{x}_{2j} - k_{1j} \cdot \frac{\tilde{x}_{1j}}{\varepsilon_{oj}} - \dot{x}_d) + c_j \cdot (\hat{x}_{1j} - x_{dj}) \quad (29)$$

Differentiating (29) as

$$\dot{\hat{s}}_j = (\dot{\hat{x}}_{2j} - k_{1j} \cdot \frac{\dot{\tilde{x}}_{1j}}{\varepsilon_{oj}} - \ddot{x}_d) + c_j \cdot (\dot{\hat{x}}_{1j} - \dot{x}_{dj}) \quad (30)$$

Substituting (9), (10), and (13) in (30) will result in (20). Now the control variable $\overline{u}$ will enforce $\hat{s}_j \cdot \dot{\hat{s}}_j \leq 0$. Hence, substituting (21) in (20) will result in

$$\dot{\hat{s}} = \alpha_3 \cdot \left\{\frac{1}{\alpha_3}\left[-K \cdot \mathrm{sat}(\hat{s}) + \tilde{d}_{2,1}\left\{\frac{k_2}{\varepsilon_o} + \frac{c \cdot k_1}{\varepsilon_o} - \frac{k_1^2}{{\varepsilon_o}^2}\right\} - c_j\{\hat{d}_{2,2} - \dot{d}_{2,d}\} + \ddot{d}_{2,d} - \hat{\psi}_2\right]\right\} - \left\{\frac{k_1}{\varepsilon_o}\right\}\tilde{d}_{2,2} - \tilde{d}_{2,1}\left\{\frac{k_2}{\varepsilon_o} + \frac{c \cdot k_1}{\varepsilon_o} - \frac{k_1^2}{{\varepsilon_o}^2}\right\} + c_j\{\hat{d}_{2,2} - \dot{d}_{2,d}\} - \ddot{d}_{2,d} + \hat{\psi}_2 \quad (31)$$

Solving (31) will subsequently result in (32)

$$\dot{\hat{s}}_j = -K_j \cdot \mathrm{sat}(\hat{s}_j) - \frac{k_{1j}}{\varepsilon_{oj}}\tilde{x}_{2j} \quad (32)$$

So, the Lyapunov function takes the following form

$$\hat{s}_j \cdot \dot{\hat{s}}_j = \left[\left(\hat{x}_{2j} - k_{1j} \cdot \frac{\tilde{x}_{1j}}{\varepsilon_{oj}} - \dot{x}_d\right) + c_j \cdot (\hat{x}_{1j} - x_{dj})\right] \cdot \left[-K_j \cdot \mathrm{sat}(\hat{s}_j) - \frac{k_{1j}}{\varepsilon_{oj}}\tilde{x}_{2j}\right] < 0 \quad (33)$$

The switching control $\left(K_j \cdot \mathrm{sat}(\hat{s}_j)\right)$ will ensure sliding convergence. Therefore, the (33) takes the following form

$$\left|\left(\hat{x}_{2j} - k_{1j} \cdot \frac{\tilde{x}_{1j}}{\varepsilon_{oj}} - \dot{x}_d\right) + c_j \cdot (\hat{x}_{1j} - x_{dj})\right| \cdot \left[-K_j \cdot \mathrm{sat}(\hat{s}_j) - \frac{k_{1j}}{\varepsilon_{oj}}\tilde{x}_{2j}\right] < 0 \quad (34)$$

It is assumed that the estimation error is bounded by $|\tilde{x}_{2j}| \leq k_{1j}$. So, to ensure $\hat{s}_j \cdot \dot{\hat{s}}_j < 0$, the selection of control gain inside the manifold $|\hat{s}_j| \leq \varepsilon_{cj}$ is

$$K_j \geq \frac{k_{1j}^2}{\varepsilon_{oj}} \quad (35)$$

Furthermore, for the desired controller parameter selection, With the conditions $|\hat{s}_j| \leq \varepsilon_{cj}$, (34) takes the following form

$$-K_j \cdot \frac{|\hat{s}_j|}{\varepsilon_{cj}} - \frac{k_{1j}}{\varepsilon_{oj}}|\tilde{x}_{2j}| < 0 \quad (36)$$

Using the coefficient relation in (23), (35) can be rewritten as

$$-\lambda_d \cdot |\hat{s}_j| - 3\lambda_d|\tilde{x}_{2j}| < 0 \quad (37)$$

(35) can be simplified as

$$-|\hat{s}_j| - 3|\tilde{x}_{2j}| < 0 \quad (38)$$

With and $|\tilde{x}_{2j}| \leq k_{1j}$, (38) becomes

$$-|\hat{s}_j| - 3k_{1j} < 0 \quad (39)$$

Again from (23), (39) can be updated as

$$-|\hat{s}_j| - 9\lambda_d\varepsilon_{oj} < 0 \quad (40)$$

As the controller tends to converge the estimated sliding surface to zero from (40), the selection of λ_d it takes the following form.

$$\lambda_d > \frac{|\hat{s}_j|}{9\varepsilon_{oj}} \quad (41)$$

Extremum Seeking

Convergence and stability of ES are affected by the selection of γ, α, and the shape of the cost function. Now to analyze the convergence of ES, considering the scalar case of $\lambda_d(k)$ and $\hat{\lambda}_d(k)$ with only one dither signal $\alpha\cos(\omega k)$. N. J. Killingsworth *et al.* assumed a quadratic cost function [15] as

$$J(.) = {f_{es}}^* + \frac{f_{es}''}{2}({\lambda_d}^* - \lambda_d)^2 \quad (42)$$

where f_{es} is positive. Taking $\tilde{\lambda}_d = {\lambda_d}^* - \hat{\lambda}_d$. And evaluated the following relation of ES dynamics error by expanding (42), filtering to remove the dc components, demodulation, and then low pass filtering [15] as

$$\tilde{\lambda}_d(k+1) \approx \left(1 - \frac{\gamma\alpha^2 f''}{2}\right)\tilde{\lambda}_d(k) \quad (43)$$

This implies that the estimation error decays exponentially. The gains γ, and α are selected, such as the positive quantity $\frac{\gamma\alpha^2 f''}{2} < 1$.

C. Selection of Cost Function

Based on (23), (16) can be rewritten as

$$\ddot{\tilde{x}}_{2j} + \lambda_d \, \tilde{x}_{2j} = \tilde{\psi}_j \tag{44}$$

Taking Laplace of (44) will result in the low pass filter transfer function with a cutoff frequency λ_d as

$$\frac{\tilde{x}_2}{\tilde{\psi}} = \frac{1}{s+\lambda_d} \tag{45}$$

Consequently, increasing λ_d will increase the breaking frequency of the low pass filter. The objective of the control algorithm is to minimize the error dynamics and converge to zero. Therefore, considering (41) and (45), the cost function for λ_d is proposed consisting of the estimated position and velocity error as in sliding surface and error dynamics as

$$J(.) = \left(w_1 \cdot \dot{\hat{e}}_j + w_2 \cdot \hat{e}_j + w_3 \cdot \tilde{x}_2\right)^2 \tag{46}$$

$w_1 = 0.1$, $w_2 = 0.8$, and $w_3 = 0.1$ are the preferences for each term. Because SMCSPO is used as position control, more preference is given to the estimated position error. Furthermore, the cost function is then changed to time-dependent integrated square error (TISE) to enhance and boost the adaptation as

$$J(.) = \frac{1}{t_2 - t_1} \int_{t_1}^{t_2} t\left(w_1 \cdot \dot{\hat{e}}_j + w_2 \cdot \hat{e}_j + w_3 \cdot \tilde{x}_2\right)^2 dt \tag{47}$$

The cost function in (47) takes the error over the time interval $[t_1, t_2]$, which in the current case becomes the sampling time. The smallest time interval is assumed while considering the effect of the perturbation on sliding dynamics in (20). Therefore, if λ_d is not enough to attenuate the perturbation effect, the actual perturbation will affect the system response greatly. Therefore, in a short interval, λ_d will adapt rapidly.

IV. Results and Discussion

For the proposed algorithm evaluation, two different systems, a seven-DOF redundant manipulator [16] in simulation and a six-DOF robot manipulator Indy-7 by Neuromeka in experimentation, as presented in Fig. 2 below, were used. The current study's ES parameters are presented in Table I as follows.

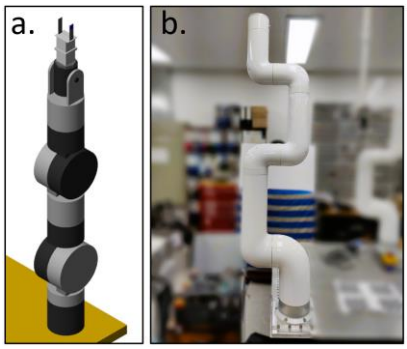

Figure 2. Robot manipulators: (a) seven-DOF, and (b) six-DOF

TABLE I. ES Parameters

Parameters				
h	ω	α	γ	dt
0.5	0.4	0.5	500	0.002

The sampling time (dt) is selected the same as the hardware. To select the modulation frequency, the fast-Fourier transform (observing joint-2) was performed with manually tuned parameters. The system was observed to have a 0.2Hz frequency when moving because of motor friction and 0.8Hz after the first sampling time. So, considering 0.8Hz, the modulation frequency is selected as half of the system frequency based on the first assumption in section III-A. For result analysis, the simulation was conducted with the initial guess of the control parameter as $\lambda_{d,\ ini} = 10$.

To understand the adaptation more clearly, the simulation was conducted iteratively (slow adaptation). After each iteration, the maximum value of λ_d is used as an initial guess for the next iteration. The simulation condition is set to achieve $mean(|\hat{e}_2|) < 0.05deg$. This is because the overall error tolerance for joint-2 is $-0.05 < mean(e_{allow}) < 0.05$. First, observing the λ_d in Fig. 3 on next page. The tuned parameters show that the initial value was very low for the system in the first iteration. Therefore, the control adapts the desired system performance abruptly. Moreover, to closely observe the behavior of λ_d, the change $\Delta\lambda_d = \lambda_{d,max} - \lambda_{d,min}$ is plotted in Fig. 4 on the next page. The value of λ_d of each iteration is subtracted from its minimum value resulting in $\Delta\lambda_d$. From the second iteration and onwards the $\Delta\lambda_d$ is very low ($\Delta\lambda_d < 1$ in the last iteration). This indicates that the λ_d is converging toward its extremum $\lambda_d{}^*$.

The mean error convergence of joint-2 is presented in Fig. 5 on the next page, which shows that after 8th iteration, the mean error becomes less than $0.05deg$. But again, after the 9th iteration, the error starts increasing. This means that now the solution is diverging away from the $\lambda_d{}^*$. The divergence is because the auto-tuned gains has exceeded the optimal value. The joint-2 trajectory tracking can be seen in Fig. 6 on the next page. In the first iteration, the maximum trajectory tracking error is 1.23, which reduced to 0.21 with optimal λ_d. The reduction of error implies that SMCSPO has enhanced the perturbation estimation, resulting in minimum or negligible perturbation estimation error. This clarifies that the system perturbation is adequately compensated.

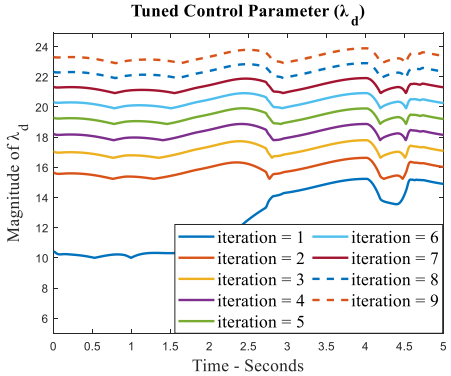

Figure 3. Tuned λ_d

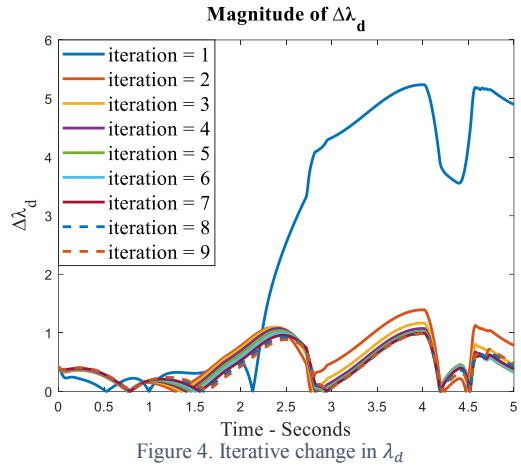

Figure 4. Iterative change in λ_d

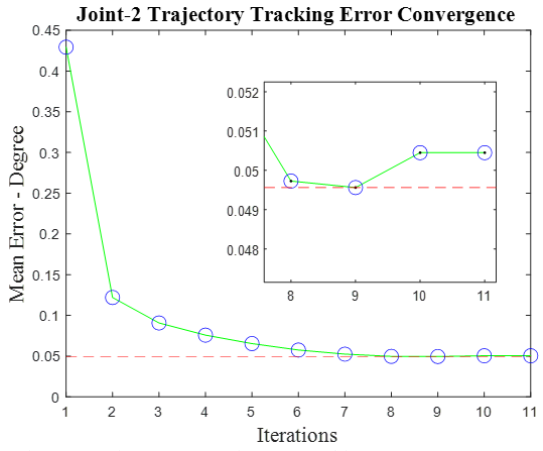

Figure 5. Joint-2 mean trajectory tracking error convergence.

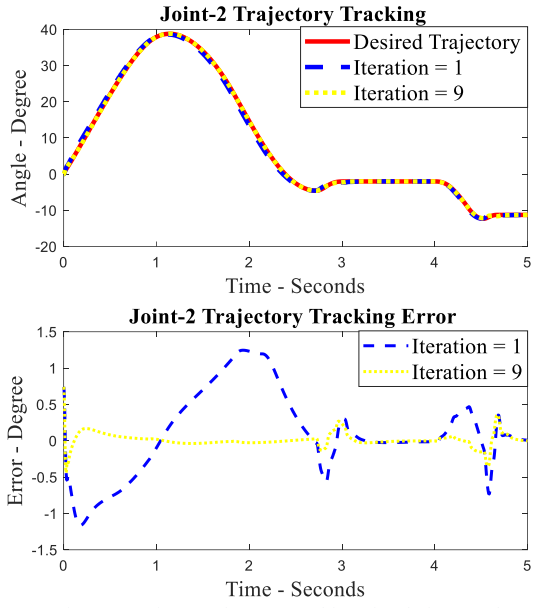

Figure 6. Joint-2 trajectory tracking simulation results

Furthermore, the proposed algorithm was evaluated based on different cost functions such as error square (ES), integrated error (IE), integrated squared error (ISE), and TISE (given in (47)) under the same conditions. The comparison is presented in Table II. The comparison shows that TISE is the best cost function for SMCSPO adaptive tuning. Moreover, $\lambda_d{}^*$ is selected by taking the average of the values in Table II, which yields $\lambda_d{}^* = 24.0043$.

TABLE II. ES-SMCSPO PERFORMANCE COMPARISON

	ES	IE	ISE	TISE
e_{mean}	0.0499	0.0501	0.0521	0.0496
$\lambda_d{}^*$	23.0951	23.5331	25.4991	23.8898
Iterations	26	15	12	9

For the experiment, observing the movement of joint-2 of the Indy-7 robot manipulator against gravity. The robot starts at the initial pose $\theta_{ini} = [45°, -45°, -45°, 0, 90°, 0°]$ and reach the home configuration $\theta_{fin} = [0°, 0°, 0°, 0, 0°, 0°]$ with a third-order polynomial trajectory in 5 seconds. The trajectory tracking error and adapted control gain is presented as follows.

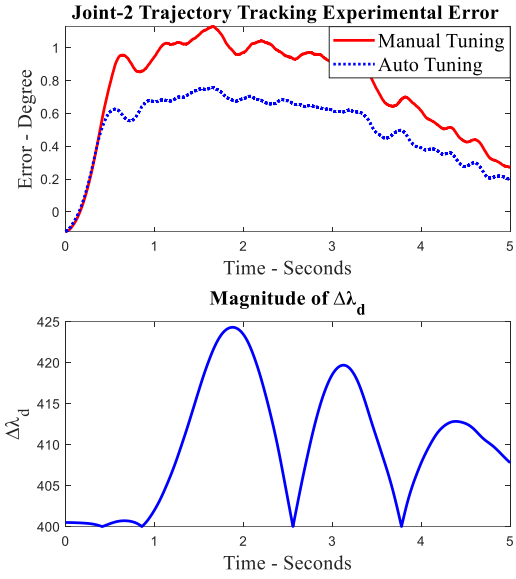

Figure 7. Joint-2 experimental results

The experimental results show that the auto-tuned controller has reduced the tracking error as compared to the manually tuned controller. This validates the proposed algorithm's effectiveness and practical implementation, which enhances trajectory tracking by achieving stability in finite time.

V. CONCLUSION

This paper proposes and investigates extremum-seeking-based adaptive sliding mode control with a sliding perturbation observer (SMCSPO). The theoretical analysis-based relationship between estimated perturbation error and sliding error dynamics of the SMCSPO was established, which is then used to propose a unique cost function for the adaptive algorithm. The cost function controls the adaptation to reduce the estimation error (enhance observer performance) and improve the tracking performance. The simulation and experimental results then validated the effectiveness of the proposed algorithm that the robust adaptive SMCSPO can precisely estimate the system states and perturbation. Consequently, the perturbation effect is well compensated from the system response, reducing the trajectory tracking error.

REFERENCES

[1] E. Abele, M. Weigold, and S. Rothenbücher, "Modeling and identification of an industrial robot for machining applications," *CIRP Annals*, vol. 56, no. 1, pp. 387-390, 2007.

[2] W. Jie, Z. Yudong, B. Yulong, H. H. Kim and M. C. Lee, "Trajectory tracking control using fractional-order terminal sliding mode control with sliding perturbation observer for a 7-dof robot manipulator," in *IEEE/ASME Transactions on Mechatronics*, vol. 25, no. 4, pp. 1886-1893, Aug. 2020.

[3] H. Obeid, L. M. Fridman, S. Laghrouche, and M. Harmouche, "Barrier function-based adaptive sliding mode control", *Automatica*, *93*, pp.540-544.

[4] S. Kumar, A. Mohammadi, D. Quintero, S. Rezazadeh, N. Gans, and R. D. Gregg, "Extremum seeking control for model-free auto-tuning of powered prosthetic legs," *IEEE Transactions on Control Systems Technology,* vol. 28, pp. 2120-2135, 2019.

[5] H. Wang, L. Fang, T. Song, J. Xu, and H. Shen "Model-free adaptive sliding mode control with adjustable funnel boundary for robot manipulators with uncertainties". *Review of Scientific Instruments*, vol. 92, no. 6, p. 065101, 2021.

[6] Y. Wang, K. Zhu, F. Yan, and B. Chen, "Adaptive super-twisting nonsingular fast terminal sliding mode control for cable-driven manipulators using time-delay estimation". *Advances in Engineering Software*, vol. 128, pp. 113-124, 2019.

[7] H. Razmi, and S. Afshinfar "Neural network-based adaptive sliding mode control design for position and attitude control of a quadrotor UAV". *Aerospace Science and Technology*, vol. 91, pp. 12-27, 2019.

[8] Z. Chen *et al*., "RBFNN-Based Adaptive Sliding Mode Control Design for Delayed Nonlinear Multilateral Telerobotic System with Cooperative Manipulation," in *IEEE Transactions on Industrial Informatics*, vol. 16, no. 2, pp. 1236-1247, Feb. 2020,

[9] R. -D. Xi, X. Xiao, T. -N. Ma and Z. -X. Yang, "Adaptive Sliding Mode Disturbance Observer Based Robust Control for Robot Manipulators Towards Assembly Assistance," in *IEEE Robotics and Automation Letters*, vol. 7, no. 3, pp. 6139-6146, July 2022.

[10] Jing, C., Xu, H., & Niu, X. "Adaptive sliding mode disturbance rejection control with prescribed performance for robotic manipulators" *ISA transactions*, vol. 91, pp. 41-51, 2019.

[11] M. Krstic and H.-H. Wang, "Stability of extremum seeking feedback for general nonlinear dynamic systems," *Automatica,* vol. 36, pp. 595-601, 2000.

[12] K. B. Ariyur and M. Krstić, *Real time optimization by extremum seeking control*: Wiley Online Library, 2003.

[13] H. Khan, S. J. Abbasi, and M. C. Lee, 'Robust position control of assistive robot for paraplegics" *International Journal of Control, Automation, and System (IJCAS),* 19, pages3741–3752, 2021.

[14] J. T. Moura, H. Elmali, and N. Olgac, "Sliding mode control with sliding perturbation observer," *Journal of Dynamic Systems, Measurement and Control,* vol. 119, no. 4, pp. 657-665, 1997.

[15] N. J. Killingsworth and M. Krstic, "PID tuning using extremum seeking: online, model-free performance optimization," *IEEE control systems magazine,* vol. 26, pp. 70-79, 2006.

[16] H. Khan, S. J. Abbasi, H. H. Kim and M. C. Lee "Robotic arm end-effector reaction force estimation for part assembling process using sliding perturbation observer" in *International Automatic Control Conference (CACS)*, 2020.